Branching fractions in singly ionized tungsten

Lennartsson, Thomas; Nilsson, Hampus; Blackwell-Whitehead, Richard; Engström, Lars; Huldt, Sven

Published in:
Journal of Physics B: Atomic, Molecular and Optical Physics

DOI:
10.1088/0953-4075/44/24/245001

2011

Branching fractions in singly ionized tungsten

2011 J. Phys. B: At. Mol. Opt. Phys. 44 245001

(http://iopscience.iop.org/0953-4075/44/24/245001)

J. Phys. B: At. Mol. Opt. Phys. **44** (2011) 245001 (6pp) doi:10.1088/0953-4075/44/24/245001

Branching fractions in singly ionized tungsten

T Lennartsson[1], H Nilsson[1], R Blackwell-Whitehead[1], L Engström[2] and S Huldt[1]

[1] Lund Observatory, Box 43, SE-221 00 Lund, Sweden
[2] Department of Physics, Lund Institute of Technology, Box 118, SE-221 00 Lund, Sweden

E-mail: thomas.lennartsson@astro.lu.se

Received 9 September 2011, in final form 7 October 2011
Published 29 November 2011
Online at stacks.iop.org/JPhysB/44/245001

Abstract
The intensity-calibrated spectra of W II have been recorded in the spectral interval 23 000–51 300 cm^{-1} (1950–4350 Å), using the FT500 UV Fourier Transform Spectrometer at Lund Observatory. Combining the intensity data in this work with lifetimes previously measured using the time-resolved laser-induced-fluorescence (TR-LIF) technique resulted in transition probabilities and log gf values for 95 transitions in W II, originating from nine different upper levels with energies between 47 179 and 55 392 cm^{-1}. Of these transitions, 85 have never been measured before. The new data are compared with theoretical calculations and with previously measured values when available.

1. Introduction

Due to the low sputtering yield, high melting point and low tritium retention, tungsten is planned to be used as a divertor material in the tokamak fusion reactor ITER. Atomic data on tungsten ions, such as emission line wavelengths and transition probabilities, are therefore needed both for diagnostic purposes and for the modelling of the fusion plasma [1].

In addition, tungsten is of interest in astrophysics. For example, neutral tungsten has been observed in 73 Drac and other Ap stars [2, 3] and its abundance has been found to be enhanced in Ba stars [4, 5]. Singly ionized tungsten was found in an Ap star in 1986 [6], although the authors stated that this observation might have been influenced by nearby lines from ions of other species. However, a line in W II was later reported in the spectrum of Sirius [7].

The most recent spectral analysis of W II was published in 2000 by Ekberg *et al* [8] where almost 2500 lines between 1800 and 5800 Å were measured and identified. In 2006 Kramida and Shirai [9] published a compilation of all observed lines in W II, together with measured absolute transition probabilities.

The first experimental transition probabilities in W II originated from arc measurements made by Corliss and Bozman in 1962 [10]. In 1973, Clawson and Miller [11] published relative transition probabilities, using a shock tube setup, and in 1983 Obbarius and Kock [12] reported new absolute values obtained from a wall-stabilized arc, operated in argon with tungsten hexafluoride. This resulted in 27 oscillator strengths that deviate from the results obtained by Corliss and Bozman [10] by up to a factor of 100. It has been pointed out that the measurements of Corliss and Bozman [10] were affected by large, systematic errors.

The main problem with the measurements by Corliss and Bozman [10] is that they depend on the assumption of local thermodynamic equilibrium (LTE), and on measurements relating to the state of the plasma, such as its electron temperature. However, combining lifetimes and branching fractions (BFs) has proven to be a reliable method for measuring absolute transition probabilities since no assumptions about the state of the plasma need to be made. In 1984, Kwiatkowski *et al* [13] published lifetimes for three levels in W II, obtained using the time-resolved laser-induced-fluorescence (TR-LIF) technique. From these lifetimes, the authors derived new absolute transition probabilities from the line intensity data from Obbarius and Kock, reducing their uncertainties by 30%. In a similar way, Henderson *et al* [14] measured lifetimes with the beam-foil method and obtained f-values by using the old intensity measurements from Corliss and Bozman.

In 2000, Kling *et al* [15] published BFs from 19 levels in W II in the wavelength range 2040–7500 Å, obtained by using a hollow cathode lamp and a Penning discharge lamp as lightsources. The BF values were combined with lifetimes measured by Schnabel *et al* [16] into absolute transition probabilities for 280 different lines (for the weakest branches, only theoretical values were given).

Recently, Nilsson *et al* [17] reported litetimes for nine energy levels between 47 179 and 55 392 cm^{-1}, measured using the TR-LIF technique. However, only calculated BFs were reported. In order to complement the work of Nilsson *et al* [17], we have measured BFs in W II for 95 lines between 1951 and 4354 Å, originating from these levels. Combining the BFs with the lifetimes reported by Nilsson *et al* [17], absolute transition probabilities are obtained.

2. Branching fractions

The branching fraction BF_{ij} is defined as

$$BF_{ij} = \frac{I_{ij}}{\sum_n I_{nj}},$$

where I_{ij} is the intensity of the transition between the lower energy level i and the upper j. Thus, to determine BF_{ij}, it is in principle necessary to measure the intensities of all transitions for level j.

2.1. Intensity measurements

In this work, we recorded the spectrum of W II between 23 000 and 51 300 cm^{-1} with a resolution of 0.05 cm^{-1}, using the Chelsea Instrument FT500 UV Fourier Transform Spectrometer at Lund Observatory. The light source was a water-cooled Penning discharge lamp with a cathode made of tungsten attached to a holder made of aluminium. Neon, at a pressure of 90 mTorr, was used as carrier gas. The current through the lamp was varied from 100 to 500 mA. To determine whether the line intensities were affected by self-absorption, we plotted ratios between two lines from the same upper level as a function of the current. All these plots gave horizontal, straight lines indicating that no self-absorption was present, and the plasma was thus regarded as optically thin. A tungsten ribbon lamp was used for intensity calibration in the interval between 23 000 and 27 500 cm^{-1}, and a deuterium lamp was used for calibration between 25 000 and 51 300 cm^{-1}. Up to 40 interferograms were added to increase the signal-to-noise ratio. The analysis was made with the program GFit [18], where the intensities were calculated by fitting Gaussian functions to the measured data. A sample of the spectra measured is shown in figure 1.

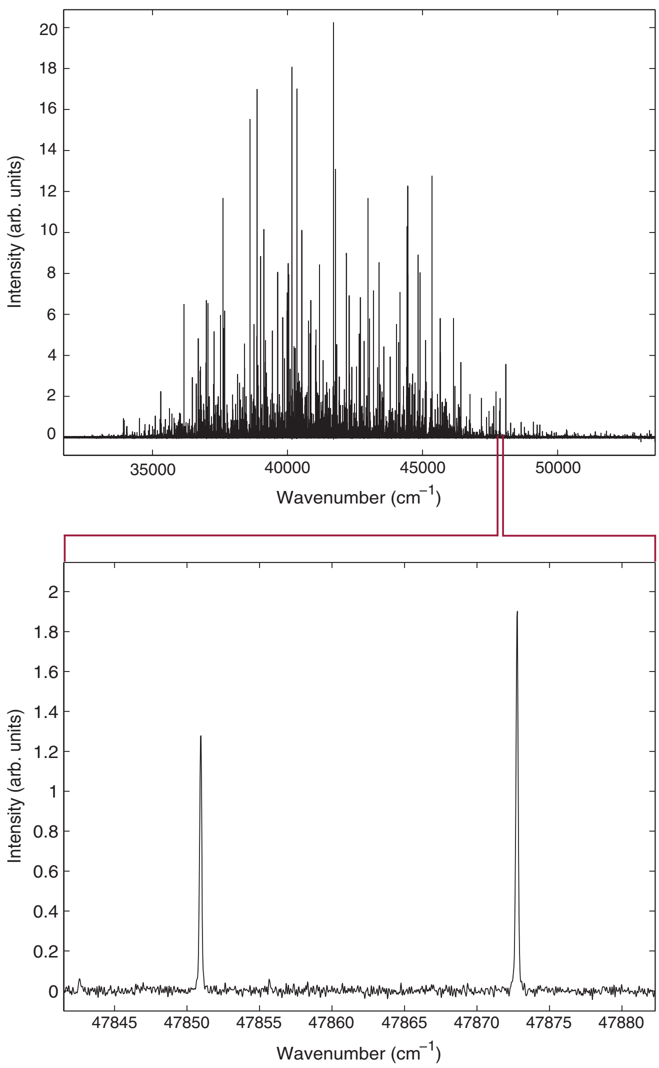

Figure 1. Sample of spectra obtained in this work. The upper part is the full spectrum from one measurement, whereas the lower part is a blow-up of a small section, containing two lines from W II.
(This figure is in colour only in the electronic version)

2.2. Transition probabilities

The transition probability A_{ij} can be derived by combining the BFs and the lifetime of the upper level τ_j:

$$A_{ij} = \frac{BF_{ij}}{\tau_j}.$$

The BFs are extracted from the intensity measurements in this work, and the lifetimes are from the work of Nilsson *et al* [17].

Using the transition probabilities A_{ij} (in s^{-1}), values of $\log gf$ have also been derived, where f_{ij} is the oscillator strength defined as

$$f_{ij} = 1.499 \times 10^{-16} \frac{g_j \lambda_{ij}^2}{g_i} A_{ij}.$$

Here λ_{ij} is the wavelength of the transition (in Ångström), g_j is the statistical weight of the upper level and g_i is the weight for the lower level.

A systematic method for quantifying the uncertainties in BF measurements has been presented by Sikström *et al* [19]. Following their method, the one-standard deviation uncertainty in the transition probability, $\sigma(A_{ij})$, is calculated through the following formula:

Table 1. Branching fractions measured in this work.

Upper level[a]	Lower level[a]	λ (Å)	BF[b]	A_{ij} (s^{-1})	Uncertainty (%)
$47\,179^{o}_{3/2}$	$0_{1/2}$	2118.874	0.364	6.28×10^{7}	5.9
	$1\,518_{3/2}$	2189.363	0.224	3.86×10^{7}	6.0
τ_k = 5.8 ns	$8\,711_{3/2}$	2598.742	0.182	3.14×10^{7}	6.1
	$8\,832_{1/2}$	2606.973	0.0451	7.78×10^{6}	6.3
	$13\,173_{1/2}$	2939.746	0.0400	6.90×10^{6}	18
	$14\,634_{3/2}$	3071.719	0.0465	8.02×10^{6}	9.3
	$16\,234_{5/2}$	3230.584	0.0150	2.59×10^{6}	13
	$18\,990_{3/2}$	3546.470	0.00594	1.02×10^{6}	18
	$19\,276_{5/2}$	3582.756	0.00424	7.31×10^{5}	18
	$22\,139_{5/2}$	3992.469	0.00529	9.12×10^{5}	13
		Residual	0.0679		
$48\,284^{o}_{5/2}$	$1\,518_{3/2}$	2137.647	0.0673	1.14×10^{7}	6.3
	$3\,172_{5/2}$	2216.014	0.237	4.02×10^{7}	5.9
τ_k = 5.9 ns	$4\,716_{7/2}$	2294.543	0.162	2.75×10^{7}	6.0
	$7\,420_{5/2}$	2446.386	0.318	5.39×10^{7}	5.8
	$8\,711_{3/2}$	2526.202	0.0166	2.81×10^{6}	7.0
	$11\,301_{5/2}$	2703.109	0.0183	3.10×10^{6}	8.2
	$13\,411_{7/2}$	2866.741	0.0269	4.56×10^{6}	14
	$14\,967_{5/2}$	3000.618	0.0232	3.93×10^{6}	11
	$18\,990_{3/2}$	3412.740	0.0365	6.18×10^{6}	10
	$20\,455_{3/2}$	3592.419	0.0177*	3.00×10^{6}	
	$23\,046_{7/2}$	3961.194	0.00378	6.41×10^{5}	13
		Residual	0.0727		
$49\,181^{o}_{9/2}$	$4\,716_{7/2}$	2248.275	0.526	2.45×10^{7}	5.5
	$6\,147_{11/2}$	2323.033	0.311	1.45×10^{7}	5.9
τ_k = 21.5 ns	$16\,553_{11/2}$	3063.966	0.0557	2.60×10^{6}	11
	$16\,589_{7/2}$	3067.400	0.0273	1.27×10^{6}	13
		Residual	0.0800		
$50\,430^{o}_{3/2}$	$0_{1/2}$	1982.907	0.143	2.17×10^{7}	20
	$3\,172_{5/2}$	2115.351	0.0641	9.71×10^{6}	9.7
τ_k = 6.6 ns	$7\,420_{5/2}$	2324.285	0.0294	4.46×10^{6}	8.1
	$8\,711_{3/2}$	2396.219	0.0588*	8.91×10^{6}	
	$8\,832_{1/2}$	2403.215	0.0226	3.42×10^{6}	6.9
	$11\,301_{5/2}$	2554.820	0.0986	1.49×10^{7}	7.1
	$13\,173_{1/2}$	2683.215	0.313	4.74×10^{7}	6.7
	$14\,967_{5/2}$	2818.990	0.0439	6.65×10^{6}	11
	$16\,234_{5/2}$	2923.439	0.0350	5.30×10^{6}	17
	$19\,637_{5/2}$	3246.482	0.0117	1.77×10^{6}	23
	$23\,450_{5/2}$	3705.313	0.0103	1.56×10^{6}	14
	$25\,045_{1/2}$	3938.101	0.00965	1.46×10^{6}	14
	$25\,169_{3/2}$	3957.532	0.00531	8.05×10^{5}	18
	$25\,672_{5/2}$	4037.813	0.00584	8.85×10^{5}	19
	$26\,226_{5/2}$	4130.364	0.00747	1.13×10^{6}	17
		Residual	0.0483		
$51\,045^{o}_{7/2}$	$3\,172_{5/2}$	2088.204	0.596	1.27×10^{8}	8.6
	$4\,716_{7/2}$	2157.797	0.183	3.89×10^{7}	9.1
τ_k = 4.7 ns	$6\,147_{11/2}$	2226.568	0.118	2.51×10^{7}	9.1
	$7\,420_{5/2}$	2291.556	0.0302	6.43×10^{6}	9.5
	$13\,411_{7/2}$	2656.427	0.0233	4.96×10^{6}	10
	$14\,967_{5/2}$	2770.987	0.0153	3.26×10^{6}	16
	$20\,780_{11/2}$	3303.203	0.00447	9.50×10^{5}	38
	$23\,450_{5/2}$	3622.831	0.00263	5.60×10^{5}	29
		Residual	0.0271		

Table 1. (Continued.)

Upper level[a]	Lower level[a]	λ (Å)	BF[b]	A_{ij} (s^{-1})	Uncertainty (%)
51 254$^{o}_{3/2}$	$0_{1/2}$	1951.051	0.233	1.11×10^{8}	18
	1 $518_{3/2}$	2009.983	0.101	4.81×10^{7}	29
τ_k = 2.1 ns	3 $172_{5/2}$	2079.118	0.1586*	7.55×10^{7}	
	7 $420_{5/2}$	2280.622	0.0903	4.30×10^{7}	11
	8 $711_{3/2}$	2349.835	0.150	7.14×10^{7}	11
	11 $301_{5/2}$	2502.161	0.0318	1.51×10^{7}	14
	13 $434_{5/2}$	2643.291	0.0841	4.01×10^{7}	11
	14 $634_{3/2}$	2729.933	0.0493	2.35×10^{7}	14
	18 $990_{3/2}$	3098.578	0.0416	1.98×10^{7}	25
	22 $139_{5/2}$	3433.722	0.0124	5.90×10^{6}	32
	22 $502_{3/2}$	3477.087	0.0232	1.11×10^{7}	20
		Residual	0.0247		
51 438$^{o}_{5/2}$	3 $172_{5/2}$	2071.208	0.334	7.26×10^{7}	9.5
	4 $716_{7/2}$	2139.655	0.0237	5.15×10^{6}	12
τ_k = 4.6 ns	7 $420_{5/2}$	2271.106	0.0354	7.70×10^{6}	9.7
	8 $711_{3/2}$	2339.733	0.0245	5.33×10^{6}	11
	11 $301_{5/2}$	2490.714	0.0888*	1.93×10^{7}	
	13 $411_{7/2}$	2628.987	0.0780	1.70×10^{7}	9.6
	13 $434_{5/2}$	2630.518	0.0242	5.26×10^{6}	10
	14 $634_{3/2}$	2716.311	0.168	3.65×10^{7}	9.5
	16 $589_{7/2}$	2868.725	0.0824	1.79×10^{7}	10
	18 $990_{3/2}$	3081.041	0.0300	6.52×10^{6}	14
	20 $039_{7/2}$	3183.956	0.0139	3.02×10^{6}	17
	22 $502_{3/2}$	3455.020	0.00880	1.91×10^{6}	17
	$23450_{5/2}$	3571.986	0.00512	1.11×10^{6}	17
	24 $804_{7/2}$	3753.610	0.00641	1.39×10^{6}	15
	25 $672_{5/2}$	3879.992	0.00266	5.78×10^{5}	20
	27 $273_{7/2}$	4137.167	0.00426	9.26×10^{5}	16
		Residual	0.0698		
54 498$^{o}_{7/2}$	4 $716_{7/2}$	2008.096	0.418	1.99×10^{8}	11
	6 $147_{11/2}$	2067.527	0.141	6.71×10^{7}	12
τ_k = 2.1 ns	7 $420_{5/2}$	2123.448	0.0154	7.33×10^{6}	19
	13 $411_{7/2}$	2433.142	0.0267	1.27×10^{7}	11
	13 $434_{5/2}$	2434.452	0.0361	1.72×10^{7}	11
	14 $967_{5/2}$	2528.909	0.0451	2.15×10^{7}	11
	16 $234_{5/2}$	2612.650	0.0413	1.97×10^{7}	11
	16 $553_{11/2}$	2634.572	0.0481	2.29×10^{7}	11
	24 $804_{7/2}$	3366.717	0.0747	3.56×10^{7}	16
	28 $118_{5/2}$	3789.707	0.00663	3.16×10^{6}	17
	31 $538_{5/2}$	4354.210	0.00634	3.02×10^{6}	18
		Residual	0.1406		
55 392 (o)	4 $716_{7/2}$	1973.314	0.0880*	3.83×10^{7}	
	6 $147_{11/2}$	2029.995	0.507	2.20×10^{8}	9.2
τ_k = 2.3 ns	13 $411_{7/2}$	2381.331	0.0285	1.24×10^{7}	9.7
	15 $146_{7/2}$	2484.002	0.0440	1.91×10^{7}	9.6
	16 $553_{11/2}$	2573.941	0.0098*	4.26×10^{6}	
	16 $589_{7/2}$	2576.359	0.0667	2.90×10^{7}	9.5
	17 $436_{11/2}$	2633.879	0.0246	1.07×10^{7}	9.9
	18 $000_{7/2}$	2673.587	0.103	4.48×10^{7}	9.5
	20 $534_{11/2}$	2867.919	0.0176	7.65×10^{6}	19
	23 $234_{11/2}$	3108.776	0.0258	1.12×10^{7}	13
	23 $803_{7/2}$	3164.769	0.0115	5.00×10^{6}	17
	23 $955_{11/2}$	3180.036	0.0270	1.17×10^{7}	13
	24 $804_{7/2}$	3268.331	0.0154	6.70×10^{6}	15
	26 $158_{11/2}$	3419.709	0.00606	2.63×10^{6}	26
	30 $632_{11/2}$	4037.709	0.00512	2.23×10^{6}	16
		Residual	0.0199		

[a] Each level is designated by the integer part of its energy value in cm^{-1} (taken from the compilation by Kramida and Shirai [9]). Odd-parity levels are denoted by 'o', values of *J* are given in subscripts.
[b] Lines marked with * are blended and the theoretical value from [17] is given.

$$\sigma(A_{ij})^2 = K_1 + K_2 + K_3 + K_4 + K_5$$
$$\equiv (1 - \mathrm{BF}_{ij})^2 \sigma(I_{ij})^2$$
$$+ \sum_{n \neq i (in A)} ((\mathrm{BF}_{nj})^2 (\sigma(I_{nj})^2 + \sigma(c_j)^2)$$
$$+ \sum_{n (in B)} ((\mathrm{BF}_{nj})^2 (\sigma(I_{nj})^2 + \sigma(c_j)^2 + \sigma(nf_{PQ})^2)$$
$$+ \sum_{n (in C)} ((\mathrm{BF}_{nj})^2 (\sigma(I_{nj})^2 + \sigma(c_j)^2 + \sigma(nf_{PQ})^2$$
$$+ \sigma(nf_{QR})^2) + \sigma(\tau_j)^2.$$

Here $\sigma(I_{ij})$ is the uncertainty of the measured line intensity as estimated from the Gaussian fitting routine in GFit. $\sigma(c_j)$, typically 5%, is the uncertainty of the intensity calibration. $\sigma(\tau)$ is the uncertainty associated with the lifetime measurements. The first term in the formula above, K_1, deals with the uncertainty in the direct measurement of the line due to the transition ij. However, the uncertainty of all other transitions from the same upper level will also contribute to $\sigma(A_{ij})$, giving rise to the terms K_2, K_3 and K_4. Due to different calibration sources and detectors, the full spectral range covered has been divided into three subranges, denoted A, B and C, covering roughly 34 000–51 300, 31 000–34 000 and 23 000–31 000 cm^{-1}, respectively. The intensities in B and C have been normalized to A since most of the strong W II lines are located in this region. However, this gives rise to additional uncertainties, $\sigma(nf_{AB})$ and $\sigma(nf_{BC})$, due to the normalization factors. It should be noted that the formula above is only valid for transitions in region A; however, it can easily be modified for B and C by cyclic permutation. Except for the weakest transitions, it is found that the uncertainty in the lifetime measurements, typically between 5% and 9%, dominates over the other terms.

From each upper level, there is generally a number of transitions that are too weak to be measured. The total transition probability of these lines has instead been estimated from the theoretical results in Nilsson *et al* [17]. Thus, it is assumed that even though the theoretical BFs for individual lines might differ from the experimental ones, the sum of all the missing lines should be approximately the same. In a few cases where the line intensities could not be measured because of blending with lines from other transitions, the theoretical results in Nilsson *et al* [17] have also been used. The uncertainty of these lines and the missing lines is set to 50%.

3. Results and discussion

The measured values of A_{ij}, sorted by upper level, are reported in table 1. Table 2 gives the corresponding log gf-values, sorted by wavelength. Lines which have not been able to be measured because of blending are marked with * in the tables. The sum of the lines too weak to be measured—the residual—is given at the end of each group of branches in table 1. These are typically between 0.02 and 0.08, with one exception: the group for 54 498 cm^{-1} have a residual of 0.14. This is due to a relatively strong transition at 1948.3253 Å which could not be measured due to heavy air absorption.

Table 2. log gf-values measured in this work.

λ (Å)	log gf[a]	λ (Å)	log gf[a]	λ (Å)	log gf[a]
1951.051	−0.60	2490.714	−0.98*	3164.769	−1.12
1973.314	−0.68*	2502.161	−1.25	3180.036	−0.75
1982.907	−1.29	2526.202	−1.79	3183.956	−1.56
2008.096	−0.02	2528.909	−0.78	3230.584	−1.79
2009.983	−0.93	2554.820	−1.23	3246.482	−1.95
2029.995	0.13	2573.941	−1.40*	3268.331	−0.97
2067.527	−0.46	2576.359	−0.54	3303.203	−1.91
2071.208	−0.55	2598.742	−0.90	3366.717	−0.32
2079.118	0.50*	2606.973	−1.50	3412.740	−1.19
2088.204	−0.18	2612.650	−0.79	3419.709	−1.34
2115.351	−1.58	2628.987	−0.98	3433.722	−1.38
2118.874	−0.77	2630.518	−1.49	3455.020	−1.69
2123.448	−1.40	2633.789	−0.95	3477.087	−1.09
2137.647	−1.33	2634.572	−0.72	3546.470	−2.11
2139.655	−1.67	2643.291	−0.77	3571.986	−1.89
2157.797	−0.66	2656.427	−1.38	3582.756	−2.25
2189.363	−0.95	2673.587	−0.32	3592.419	−1.57*
2216.014	−0.75	2683.215	−0.69	3622.831	−2.05
2226.568	−0.83	2703.109	−1.69	3705.313	−1.89
2248.275	−0.73	2716.311	−0.62	3753.610	−1.75
2271.106	−1.45	2729.933	−0.98	3789.707	−1.26
2280.622	−0.87	2770.987	−1.52	3879.992	−2.11
2291.556	−1.39	2818.990	−1.50	3938.101	−1.87
2294.544	−0.89	2866.741	−1.47	3957.532	−2.12
2323.033	−0.93	2867.919	−1.03	3961.194	−2.04
2324.285	−1.84	2868.725	−0.88	3992.469	−2.06
2339.733	−1.58	2923.439	−1.57	4037.709	−1.26
2349.835	−0.63	2939.746	−1.45	4037.813	−2.06
2381.331	−0.98	3000.618	−1.50	4130.364	−1.94
2396.219	−1.42*	3063.966	−1.44	4137.167	−1.85
2403.215	−1.93	3067.400	−1.75	4354.210	−1.16
2433.142	−1.05	3071.719	−1.34		
2434.452	−0.91	3081.041	−1.25		
2446.386	−0.54	3098.578	−0.94		
2484.002	−0.75	3108.776	−0.79		

[a] Lines marked with * are blended and the theoretical value from [17] is given.

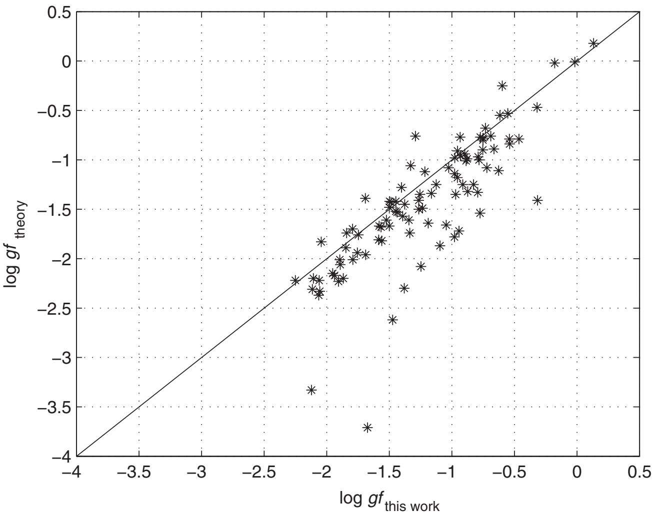

Figure 2. Comparison between log gf-values measured in this work and the theoretical values calculated by Nilsson *et al* [17].

The wavelengths and wavenumbers given in the tables have been taken from the compilation by Kramida and Shirai

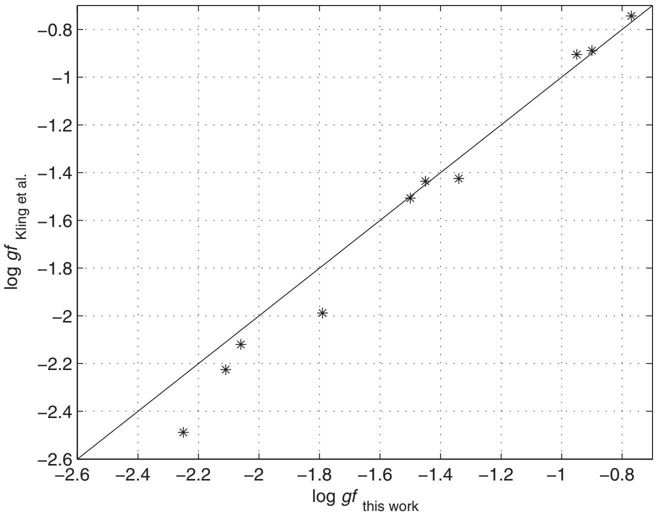

Figure 3. Comparison between log gf-values measured in this work and previously measured values by Kling *et al* [15].

[9]. A comparison of the measured values and the ones calculated by Nilsson *et al* [17] shows good agreement, as can be seen in figure 2. A few experimental log gf values deviate considerably from the calculated values; even though they are quite weak, this deviation is too large to be explained by uncertainties due to low signal to noise. When $\log gf_{\text{exp}} > \log gf_{\text{theory}}$, one possibility is that line blending increases the apparent intensity. This has been thoroughly investigated and no such (known) lines have been found. It should be noted that W II is a system where the amount of level mixing is very high. As an example the 50 $430_{3/2}$ state can be considered, where the three strongest eigenvector components are mixed with the distributions of 14%, 11% and 10% [8]. This might lead to difficulties when calculating the BFs, especially for the weakest transitions.

For the branches originating from the level of 47 179 cm^{-1}, Kling *et al* [15] have made similar measurements and a comparison with these shows a good correspondence, which can be seen in figure 3.

Acknowledgments

TL would like to acknowledge funding from Swedish Energy Agency grant P3015-2. RBW gratefully acknowledges the European Commission for a Marie Curie fellowship. HN acknowledges the support of the Linneaus grant to the Lund Laser Centre from the Swedish Research Council.

References

[1] Skinner C H 2009 *Phys. Scr.* T **134** 014022
[2] Jaschek M and Brandi E 1972 *Astron. Astrophys.* **20** 233
[3] Guthrie B N G 1972 *Astrophys. Space. Sci.* **15** 214
[4] Warner B 1965 *Mon. Not. R. Astron. Soc.* **129** 263
[5] Danziger I R 1965 *Mon. Not. R. Astron. Soc.* **131** 51
[6] Hensberge H, Van Santvoort J, van der Hucht K A and Morgan T H 1986 *Astron. Astrophys.* **158** 113
[7] Sadakane K 1991 *Publ. Astron. Soc. Pac.* **103** 355
[8] Ekberg J O, Kling R and Mende W 2000 *Phys. Scr.* **61** 146
[9] Kramida A E and Shirai T 2006 *J. Phys. Chem. Ref. Data* **35** 423
[10] Corliss C H and Bozman W R 1962 *Experimental Transition Probabilities for Spectral Lines of Seventy Elements* (Washington, DC: National Bureau of Standards)
[11] Clawson J E and Miller J 1973 *J. Opt. Soc. Am.* **63** 1598
[12] Obbarius H U and Kock M 1982 *J. Phys. B: At. Mol. Phys.* **15** 527
[13] Kwiatkowski M, Naumann F, Werner K and Zimmermann P 1984 *Phys. Lett.* A **103** 49
[14] Henderson M, Irving R E, Matulioniene R, Curtis L J, Ellis D G, Wahlgren G M and Brage T 1999 *Astrophys. J.* **520** 805
[15] Kling R, Ekberg J O and Kock M 2000 *J. Quant. Spectrosc. Radiat. Transfer* **67** 227
[16] Schnabel R, Schultz-Johanning M and Kock M 1998 *Eur. Phys. J.* D **5** 341
[17] Nilsson H, Engström L, Lundberg H, Palmeri P, Fivet V, Quinet P and Biémont É 2008 *Eur. Phys. J.* D **49** 13
[18] Engström L 1998 *Lund Reports on Atomic Physics* LRAP-232 (http://kurslab-atom.fysik.lth.se/Lars/GFit/html/index.html)
[19] Sikström C M, Nilsson H, Litzén U, Blom A and Lundberg H 2002 *J. Quant. Spectrosc. Radiat. Transfer* **74** 355